

## Pairing from strong repulsion in triangular lattice Hubbard model

Shang-Shun Zhang,<sup>1</sup> Wei Zhu,<sup>2</sup> and Cristian D. Batista<sup>1,3</sup><sup>1</sup>Department of Physics and Astronomy, University of Tennessee, Knoxville, Tennessee 37996-1200, USA<sup>2</sup>Theoretical Division, T-4 and CNLS, Los Alamos National Laboratory, Los Alamos, New Mexico 87545, USA<sup>3</sup>Quantum Condensed Matter Division and Shull-Wollan Center, Oak Ridge National Laboratory, Oak Ridge, Tennessee 37831, USA

(Received 8 November 2017; revised manuscript received 22 January 2018; published 20 April 2018)

We propose a pairing mechanism between holes in the dilute limit of doped frustrated Mott insulators. Hole pairing arises from a hole-hole-magnon three-body bound state. This pairing mechanism has its roots on single-hole kinetic energy frustration, which favors antiferromagnetic (AFM) correlations around the hole. We demonstrate that the AFM polaron (hole-magnon bound state) produced by a single hole propagating on a field-induced polarized background is strong enough to bind a second hole. The effective interaction between these three-body bound states is repulsive, implying that this pairing mechanism is relevant for superconductivity.

DOI: [10.1103/PhysRevB.97.140507](https://doi.org/10.1103/PhysRevB.97.140507)

The long-sought resonating valence bond superconductor [1,2] was the germ of two fundamental ideas in modern condensed-matter physics. Besides setting the basis for finding quantum spin liquid states in Mott insulators, it suggested a clear connection between geometric frustration and superconductivity. The new century is witnessing an explosion of works based on the first idea [3]. The superconductivity found in two-dimensional CoO<sub>2</sub> layers [4] also triggered efforts to test the second idea [5–9]. However, the relationship between frustration and superconductivity remains much less explored.

Nagaoka's theorem reveals a striking interplay between magnetism and electronic kinetic energy in slightly doped Mott insulators [10,11]. The theorem states that a single hole propagating on a  $D$ -dimensional ( $D > 1$ ) bipartite lattice with infinite on-site Hubbard repulsion  $U$  minimizes its kinetic energy in a ferromagnetic (FM) background. This result motivated the so-called “spin-bag” pairing mechanism [12]: a single hole propagating on a bipartite antiferromagnet generates a FM spin-bag inside which the hole is self-consistently trapped. Two holes are attracted by sharing a common bag. While never confirmed, this idea gives an interesting angle on understanding how attraction can arise from bare repulsion.

As shown in Fig. 1(a) for a square lattice and nearest-neighbor (NN) hopping  $t_1$ , the single-hole kinetic energy ( $-4|t_1|$ ) is minimized in a uniform FM background because the interference between different paths connecting two given points is always *constructive*. The situation is very different for nonbipartite structures, such as the triangular lattice [13–15]. The single-hole kinetic energy is now frustrated if the product of three hopping matrix elements of one triangle is *positive*. For instance, the minimum kinetic energy of a single hole on a triangular lattice is  $-3|t_1|$  for a uniform FM background if the kinetic energy is frustrated ( $t_1 > 0$ ) [see Fig. 1 (b)], while it is  $-6|t_1|$  in absence of frustration ( $t_1 < 0$ ). Frustration arising from *destructive* interference between different paths can be avoided if the uniform FM background is replaced with a nonuniform state where one or more spins are flipped. As shown in Fig. 1(c), hole paths no longer interfere if one path goes through a flipped spin [13–15].

In this Rapid Communication we demonstrate that kinetic frustration is also the source of hole pairing near the magnetic field-induced fully polarized state. Below the saturation field,  $H_{\text{sat}}$ , it is energetically convenient to flip at least one spin. A single hole can then lower its kinetic energy by remaining close to a flipped spin. The resulting hole-magnon bound state, or AFM polaron [16], has a binding energy  $\sim -|t_1|/2$ , i.e., the lowest single-polaron kinetic energy can reach a value as low as  $-3.5|t_1|$ , which must be compared against  $-3|t_1|$  (magnons have infinite mass for  $U \rightarrow \infty$ ). Remarkably, the AFM polaron mass,  $m_p \simeq 10/|t_1|$ , still has a moderate value. If a second hole is present, the strong hole-magnon attraction also leads to a *three-body bound state*, or AFM bipolaron, which still has an effective mass of order  $10/|t_1|$ . Moreover, our density matrix renormalization group (DMRG) results reveal a repulsive interaction between AFM bipolarons, implying that they should condense in the dilute limit.

We start by considering a Hubbard model on a triangular lattice with NN hopping  $t_1$  and third NN hopping  $t_3$ :

$$\mathcal{H}_H = -t_1 \sum_{\langle ij \rangle_{1\sigma}} c_{i\sigma}^\dagger c_{j\sigma} - t_3 \sum_{\langle ij \rangle_{3\sigma}} c_{i\sigma}^\dagger c_{j\sigma} - \mu \sum_i n_i + U \sum_i n_{i\uparrow} n_{i\downarrow} - H \sum_i S_i^z, \quad (1)$$

where  $n_\sigma(\mathbf{r}) = c_{r\sigma}^\dagger c_{r\sigma}$  and  $\mu$  is the chemical potential. We will initially consider the  $U/|t_1| \rightarrow \infty$  limit. The ground state is fully polarized for  $H > H_{\text{sat}}$ . In this regime the holes become noninteracting fermions with dispersion  $\epsilon_{\mathbf{k}} = 2t_1[\cos(2k_x/\sqrt{3}) + 2\cos(k_x/\sqrt{3})\cos(k_y)] + 2t_3[\cos(4k_x/\sqrt{3}) + 2\cos(2k_x/\sqrt{3})\cos(2k_y)]$ . For  $t_3 = 0$  the minimum of  $\epsilon_{\mathbf{k}}$  is  $\epsilon_0 = -6|t_1|$  for  $t_1 < 0$  and  $\epsilon_{\pm\mathbf{K}} = -3|t_1|$  for  $t_1 > 0$  (frustrated case [17]) with  $\mathbf{K} = (\frac{4\pi}{3}, 0)$ . A finite  $t_3$  changes the degree of kinetic energy frustration [18].

*AFM polaron.* The single-hole ground state is no longer fully polarized for  $H < H_{\text{sat}} = -\Delta_b^{h-m}$ , where  $\Delta_b^{h-m}$  is the hole-magnon binding state energy. This bound state forms to suppress the destructive interference (frustration) of the single-hole motion, a phenomenon that can be illustrated with a simple

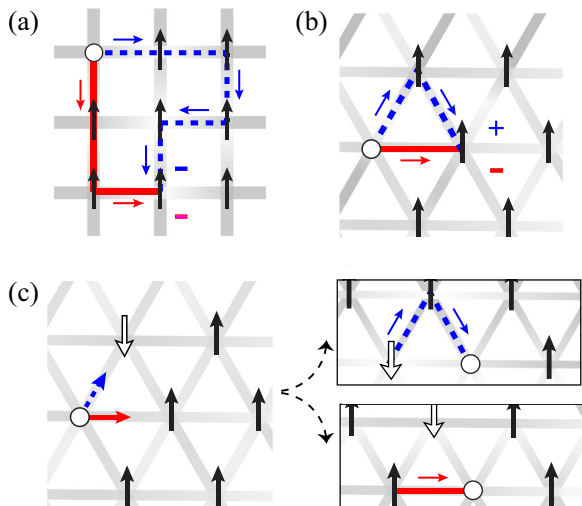


FIG. 1. Single-hole propagation in fully polarized (a) square and (b) triangular lattices with  $t_1 > 0$ . The signs indicate the optimal phase factor for each path. (c) Lack of destructive interference when one of the paths goes through a flipped spin.

variational wave function for the relative coordinate  $\mathbf{r}$  of the hole-magnon pair:

$$\psi(\mathbf{r}) = \frac{\cos \alpha}{\sqrt{6}} e^{im\theta} \delta_{|\mathbf{r}|,a} + \frac{\sin \alpha}{\sqrt{6}} e^{i(m\theta+\phi)} \delta_{|\mathbf{r}|,2a}. \quad (2)$$

Here,  $m = 0, \dots, 5$  is the crystal angular momentum following from the  $C_6$  symmetry of  $\mathcal{H}_H$ ,  $\theta = n\pi/3$  ( $0 \leq n \leq 5$ ) is the relative azimuthal angle and  $\phi$  is the phase difference between the two particles separated by one and two lattice spaces  $a$ . Minimization of the variational energy  $E(\alpha) = t_1 \{(\cos \alpha)^2 [2 \cos(\frac{m\pi}{3}) + \cos(m\pi)] + \sin 2\alpha \cos(\phi)\} + t_3 [2 \sin^2 \alpha \cos(\frac{m\pi}{3}) + \cos(m\pi)]$  for zero momentum of the two-particle system and  $t_1 > 0$ ,  $t_3 > -0.75t_1$  gives  $m = 3$  and  $\phi = \pi$ . For  $t_3 = 0$ , we obtain  $\cos \alpha = 0.3907$  and  $\tilde{E}_{\min} = -3.3028t_1$ , which is close to the exact ground-state energy  $E_G = -3.4227t_1$  obtained by solving the Lippmann-Schwinger equation in the thermodynamic limit [19]. The binding energy,  $\min_{\mathbf{k} \in \text{BZ}}(\epsilon_{\mathbf{k}}) - E_G$ , is  $0.4227t_1$ , indicating a strong hole-magnon attraction. The correlation function  $c^{h-m}(\mathbf{r}) = \sum_{\mathbf{r}'} \langle n_h(\mathbf{r} - \mathbf{r}') n_\downarrow(\mathbf{r}') \rangle$ , shown in Fig. 2(b), reveals the real-space distribution of the magnon around the hole for the exact ground state.

The lowest energy magnon-hole pair can also have finite momentum. Figure 2(c) shows the exact binding energy,  $\Delta_b^{h-m} = E(1H1S) - E(1H) - E(1S)$ , as a function of  $t_3/|t_1|$  that results from solving the Lippmann-Schwinger (LS) equation in the thermodynamic limit [19]. For  $t_3 < -0.1615t_1$ , the lowest energy bound state is at the  $M$  point of the Brillouin zone (BZ). The center-of-mass momentum of the ground state moves from the  $M$  to the  $\Gamma$  point for  $t_3 > -0.1615|t_1|$ . A positive  $t_3$  does not change the nature of the bound state, which smoothly crosses over into another limit dominated by  $t_3$  [20].

From now on, we will adopt the notation  $mHnS$  to denote states with  $m$  holes and  $n$  flipped spins. We will first consider bound states of one hole ( $m = 1$ ) and  $n \geq 1$  flipped spins. Figure 3(a) shows the  $H$ - $t_3/t_1$  phase diagram. The  $1H1S$  is stable over a relatively large window of magnetic field values

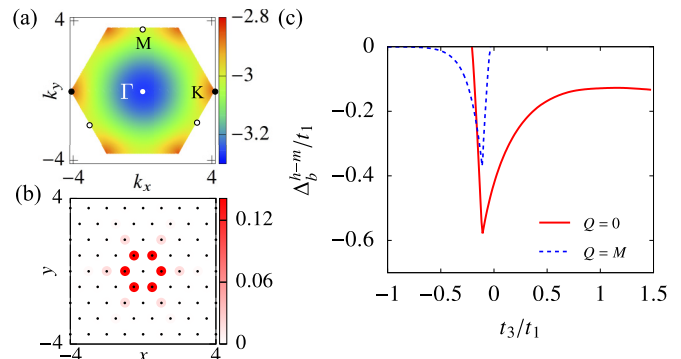


FIG. 2. (a) Dispersion relation of the hole-magnon bound state with minimum at the  $\Gamma$  point for  $t_3 = -0.1t_1$ . (b) Correlation function between the hole and the magnon  $c^{h-m}(\mathbf{r}) = \sum_{\mathbf{r}'} \langle n_h(\mathbf{r} - \mathbf{r}') n_\downarrow(\mathbf{r}') \rangle$  for the lowest energy bound state at the  $\Gamma$  point. (c) Binding energy of the hole-magnon bound state  $\Delta^{h-m} = E_g(1H1S) - E_g(1H) - E_g(1S)$  as a function of  $t_3/t_1$ .

for small  $|t_3|/t_1 \lesssim 0.1$ . The number of magnons bounded to the hole increases continuously upon further decreasing  $H$ , and the critical field for the transition into a  $1HnS$  state decreases rapidly with  $n$  because the binding energy of the  $n$ th magnon goes asymptotically to zero for  $n \rightarrow \infty$ . This AFM polaron state is then expected to evolve smoothly into the long-range AFM ordering found in Ref. [13] for  $h \rightarrow 0$  ( $n \rightarrow \infty$ ) because the radius of the AFM polaron (AFM correlation length) diverges. Figure 3(b) shows  $c^{h-m}(\mathbf{r})$  as a function of  $n$  for  $n = 1, 2, 3$ . For  $n \leq 3$ , the radius of the AFM polaron turns out to be significantly smaller than the linear size of the biggest lattices that enable exact diagonalization (ED) of  $\mathcal{H}_H$ .

*Hole pairing.* The effective hole-magnon attraction enables indirect hole-hole pairing via formation of a *three-body bound state of two holes and one magnon (2H1S)*. This state can be regarded as an AFM “bipolaron” or spin bag: the two holes share the same AFM region to lower their kinetic energy at a minimum Zeeman energy cost. Its wave function is also obtained by solving the LS equation in the thermodynamic limit [19], which gives a reference to quantify the size effects of ED and DMRG calculations on finite lattices [19].

The two holes and the magnon indeed form a tight bound state for  $t_1 > 0$ . The lowest energy  $2H1S$  bound state has

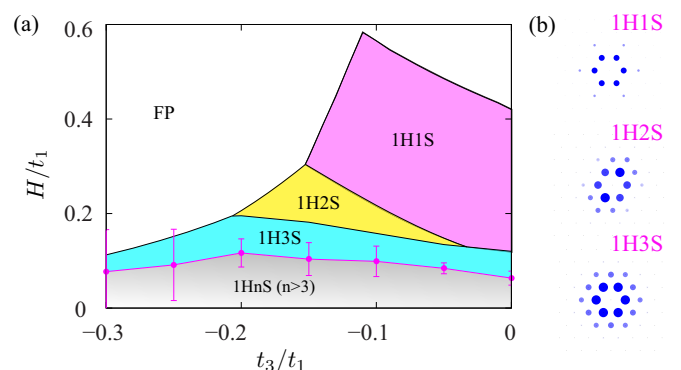


FIG. 3. (a) Phase diagram of one hole system on the  $t_3$ - $H$  plane with  $t_1 > 0$ . The gray region has stronger finite-size effects. (b) Correlation function between the hole and the magnon  $c^{h-m}(\mathbf{r})$  for different number of flipped spins ( $t_3 = -0.1t_1$ ).

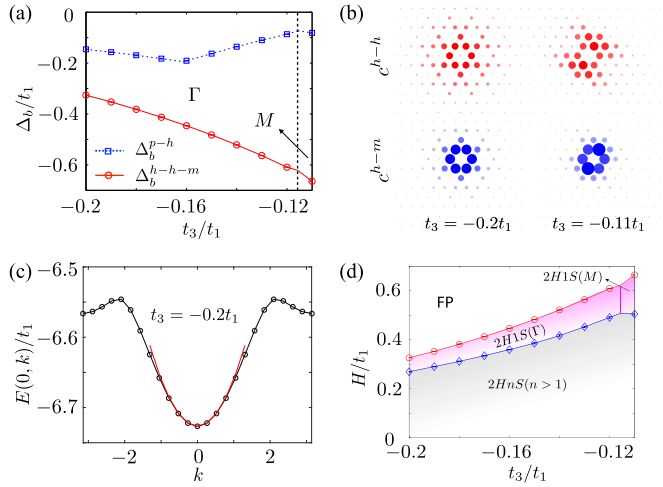


FIG. 4. (a) Binding energies  $\Delta_b^{p-h} = E_g(2H1S) - E_g(1H1S) - E_g(1H)$  and  $\Delta_b^{h-h-m} = E_g(2H1S) - 2E_g(1H) - E_g(1S)$  as a function of  $t_3/t_1$ . The two kinks of  $\Delta_b^{p-h}$  arise from a change in the center-of-mass momentum of the AFM polaron (at  $t_3 = 0.175t_1$ ) and the AFM bipolaron (at  $t_3 = 0.11t_1$ ). (b) Hole-hole,  $c^{h-h}(\mathbf{r})$  and hole-magnon,  $c^{h-m}(\mathbf{r})$ , correlation functions for different values of  $t_3/t_1$  ( $L = 26$ ). (c) Dispersion relation of the bipolaron ( $2H1S$  bound state) for  $t_3 = -0.2t_1$  obtained from solving the LS equation (line) and from ED of an  $L \times L$  lattice with  $L = 24$  (circles). The effective mass,  $m_{2H1S}$ , is extracted by fitting the long-wavelength region with a parabola. (d) Stability region of  $2H1S$  state in the  $H$ - $t_3/t_1$  phase diagram ( $U \rightarrow \infty$  limit).

center-of-mass momentum  $\mathbf{Q} = \mathbf{0}$  for  $t_3 < -0.116t_1$  ( $t_1 > 0$ ). The binding energy between a  $1H1S$  polaron and a second hole is defined as  $\Delta^{p-h} = E_g(2H1S) - E_g(1H1S) - E_g(1H)$ . It is also useful to introduce the binding energy of the three-body bound state relative to three noninteracting particles:  $\Delta^{h-h-m} = E_g(2H1S) - 2E_g(1H) - E_g(1S)$ . Both binding energies are shown in Fig. 4(a). The negative value of  $\Delta^{p-h}$  demonstrates the AFM bipolaron formation, as confirmed by the hole-hole,  $c^{h-h}(\mathbf{r}) = \sum_{\mathbf{r}'} \langle n_h(\mathbf{r} - \mathbf{r}') n_h(\mathbf{r}') \rangle$ , and the hole-magnon,  $c^{h-m}(\mathbf{r})$ , correlation functions shown in Fig. 4(b). Figure 4(c) includes the AFM bipolaron dispersion relation for  $t_3 = -0.2t_1$ , from which we extract an effective mass  $m_{2H1S} \simeq 9.91t_1^{-1}$ . The center-of-mass momentum of the lowest energy bound state moves to the  $\mathbf{M}$  point of the BZ for  $-0.116t_1 < t_3 < -0.1t_1$ . However, the bandwidth  $W_{2H1S} \simeq 0.0737t_1$  is significantly narrower in this regime. Correspondingly, the effective mass is large and anisotropic:  $m_{2H1S}^{\parallel} \simeq 23.3t_1^{-1}$  and  $m_{2H1S}^{\perp} \simeq 66.67t_1^{-1}$  for parallel and perpendicular directions to the  $\mathbf{M}$  vector.

As shown in Fig. 4(d), a second spin flips and binds to the  $2H1S$  bound state upon further lowering  $H$ . The corresponding critical field is  $H_{2S2H}^c = -\Delta_b^{h-m}$ , where  $\Delta_b^{h-m} = E(2H2S) - E(2H1S) - E(1S)$  is the binding energy between the AFM bipolaron and the second magnon. The critical field boundary shown in Fig. 4(d) is obtained from finite-size scaling of the ground-state energy [19].

*Interaction between AFM bipolarons.* Given that hole pairs are actually  $2H1S$  bound states, we will further elucidate that AFM bipolarons interact repulsively, instead of forming larger

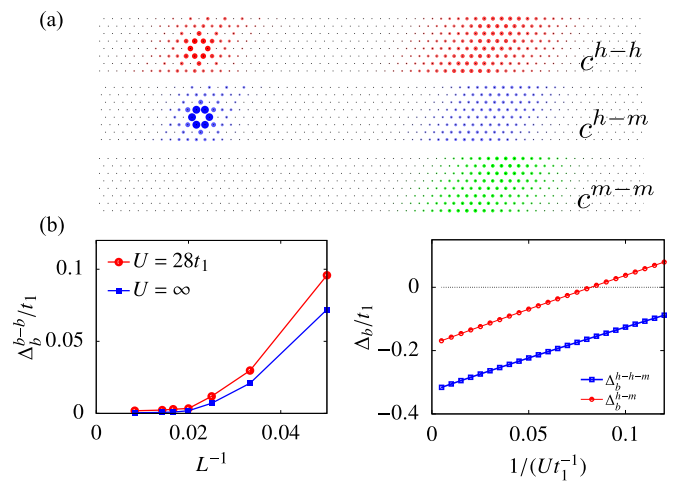


FIG. 5. Correlation functions for four holes and two magnons: (a) Hhole-hole,  $c^{h-h}(\mathbf{r})$ ; hole-magnon,  $c^{h-m}(\mathbf{r})$ ; and magnon-magnon,  $c^{m-m}(\mathbf{r})$ . The calculation is performed by DMRG simulation on an  $8 \times 120$  lattice and setting  $t_1 = 1$ ,  $t_3 = -0.2$ ,  $U = \infty$ . This result indicates that the bipolarons ( $2H1S$  bound states) are well separated. (b) Finite-size scaling of the binding energy between AFM bipolarons,  $\Delta_b^{b-b} = E(4H2S) - 2E(2H1S)$ .  $\Delta_b^{b-b}$  is positive for finite  $L$  and it extrapolates to zero in the  $L \rightarrow \infty$  limit confirming the repulsive nature of the interaction. (c) ED results: Binding energies  $\Delta_b^{h-h-m}$  and  $\Delta_b^{h-m}$  as a function of  $U$ .

bound states with multiple holes and magnons. Figure 5(a) shows the hole-hole, hole-magnon, and magnon-magnon correlation functions for the ground state of the six-body  $4H2S$  system ( $t_3/t_1 = -0.2$ ). According to this result, the particles split into well separated  $2H1S$  AFM bipolarons with the same correlation functions,  $c^{h-h}(\mathbf{r})$  and  $c^{h-m}(\mathbf{r})$ , of an individual bipolaron [see Fig. 4(b)]. The magnon density-density correlation function,  $c^{m-m}(\mathbf{r}) = \sum_{\mathbf{r}'} \langle n_{\downarrow}(\mathbf{r} - \mathbf{r}') n_{\downarrow}(\mathbf{r}') \rangle$ , confirms that each bipolaron contains one magnon. The ground-state energy  $E_g(4H2S)$  equals twice the ground-state energy of the  $2H1S$  bound state,  $E_g(4H2S) = 2E_g(2H1S)$ , within an error of order  $10^{-4}t_1$ . In addition, as shown in Fig. 5(b) for  $t_3/t_1 = -0.2$ ,  $\Delta_b^{b-b} = E_g(4H2S) - 2E_g(2H1S)$  is positive for finite  $L$  and it extrapolates to zero for  $L \rightarrow \infty$ , confirming the repulsive nature of the effective interaction. We note, however, that the two AFM bipolarons form a bound state when  $t_3/t_1$  approaches  $-0.1$  [region of strongest hole-magnon pairing according to Figs. 2(c) and 4(a)]. However, as we discuss below, the interaction between AFM bipolarons becomes also repulsive in this region for a finite  $U \lesssim 20|t_1|$ .

*Effect of spin exchange.* Our next step is to analyze the effect of a finite  $U/|t_1| \gg 1$ . The low-energy sector of the Hubbard model is now described by the  $t$ - $J$  model:

$$\begin{aligned} \mathcal{H}_{t-J} = & -t_1 \sum_{\langle ij \rangle_1} \tilde{c}_{i\sigma}^{\dagger} \tilde{c}_{j\sigma} - t_3 \sum_{\langle ij \rangle_3} \tilde{c}_{i\sigma}^{\dagger} \tilde{c}_{j\sigma} - \mu \sum_i n_i \\ & + J_1 \sum_{\langle ij \rangle_1} \mathbf{S}_i \cdot \mathbf{S}_j + J_3 \sum_{\langle ij \rangle_3} \mathbf{S}_i \cdot \mathbf{S}_j - H \sum_i S_i^z \\ & - \sum_{i \neq k} \frac{t_{ij} t_{jk}}{2U} \tilde{c}_{i\sigma}^{\dagger} \tilde{c}_{k\sigma} n_{j\bar{\sigma}} + \sum_{i \neq k} \frac{t_{ij} t_{jk}}{2U} \tilde{c}_{i\sigma}^{\dagger} \tilde{c}_{k\bar{\sigma}} \tilde{c}_{j\bar{\sigma}}^{\dagger} \tilde{c}_{j\sigma}. \quad (3) \end{aligned}$$

$J_\nu = 4t_\nu^2/U$  ( $\nu = 1, 3$ ) and  $\tilde{c}_{i\sigma}^{(\dagger)}$  are annihilation (creation) operators of constrained fermions:  $\tilde{c}_{i\sigma}^\dagger = c_{i\bar{\sigma}}^\dagger(1 - c_{i\bar{\sigma}}^\dagger c_{i\bar{\sigma}})$ . The  $XY$  part of the AFM exchange interactions,  $J_1$  and  $J_3$ , generate a finite magnon mass, while the Ising part induces a repulsive interaction between any pair of particles (magnons or holes). Consequently, a finite  $U/|t_1|$  should reduce the binding energy of the AFM polaron and bipolaron bound states. Indeed, as shown in Fig. 5(c), the AFM polaron bound state disappears below a critical value of  $U/|t_1| \simeq 12.2$ , implying that the effective hole-hole attraction decreases upon *reducing* the bare Coulomb repulsion  $U$ . Moreover, a finite  $U/|t_1|$  increases the repulsion between AFM bipolarons [see Fig. 5(b)].

*Order parameter.* Our results indicate the existence of a stable gas of AFM bipolarons for low hole concentration  $\rho_h \ll 1$  and  $H \lesssim H_{\text{sat}}$  [21]. In a pure 2D scenario, the AFM bipolarons must undergo a Berezinskii-Kosterlitz-Thouless transition [22–24] into a superfluid state at a transition temperature  $T_{\text{BKT}}$  of order  $\rho_h/m_{2H1S}$ . The real-space superconducting (SC) order parameter is  $\Delta = \langle h_i^\dagger h_j^\dagger S_k^- \rangle$ , where  $i, j, k$  are neighboring sites. Given the three-body nature of the bound state, the phase  $\theta$  of the order parameter  $\Delta$  includes a charge and a spin contribution (the superfluid current carries both charge and spin). The Hubbard Hamiltonian in a magnetic field  $\mathbf{H} = H\hat{z}$  has a  $U(1) \times U(1)$  symmetry associated with the conservation of  $\sum_j n_j$  and  $\sum_j S_j^z$ . The phase  $\theta$  is transformed into  $\theta - \theta_s$  under a global spin rotation by an angle  $\theta_s$  and into  $\theta + 2\theta_c$  under a global charge rotation by  $\theta_c$  ( $c_{j\sigma}^\dagger \rightarrow e^{-i\theta_c} c_{j\sigma}^\dagger$ ). The condensate is then invariant under the product of a spin rotation by  $2\phi$  and a charge rotation by  $\phi$  [ $U(1)$  subgroup]. This invariance implies lack of long-range magnetic ordering because the spin field can have arbitrary large phase fluctuations  $\delta\theta_s$ , which are compensated by  $\delta\theta_c$ . Magnetic order can only take place via *single magnon condensation*.

The pairing symmetry is determined by the irreducible representation of the single AFM bipolaron ( $2H1S$ ) ground state. For  $t_3/t_1 = -0.2$  ( $t_1 > 0$ ), the wave function of the  $2H1S$  bound state has zero total momentum and it belongs to the  $B_2$  representation of the  $D_6$  space group ( $f_2$  wave) [25,26].

*Discussion.* Understanding the generation of effective attraction out of the bare Coulomb repulsion is a long sought-after goal in condensed matter [27–44]. We have shown that magnons provide a strong glue even in the  $U \rightarrow \infty$  limit of a slightly doped frustrated Mott insulator. The strongly attractive hole-magnon interaction is a manifestation of the “counter-Nagaoka” mechanism [13–15]: a single hole can lower its kinetic energy by creating a hole-magnon bound state (AFM polaron). The second hole binds to the polaron (AFM bipolaron) to lower its kinetic energy at a minimum Zeeman energy cost. AFM bipolarons interact repulsively and they should therefore condense in the dilute limit.

A saturation field of order  $|t_1|/2$  is much higher than typical laboratory fields. Moreover, such a high field would produce a large orbital effect not included in our analysis. For charged systems, like electrons in a solid (e.g.,  $\text{Na}_x\text{CoO}_2$  [45]), this problem can be avoided by replacing the external field with the molecular field generated by the interaction between the moments  $\mathbf{S}_j$  and an insulating ferromagnetic layer. For neutral systems, such as atomic gases [46–50], the orbital effect is not present and the system can be easily driven into the fully polarized state. Nevertheless, the main purpose of our analysis is to understand how magnetic excitations can provide the glue for hole-hole pairing in the vicinity of a field-induced AFM quantum critical point of the finite- $U$  Mott insulator. Remarkably, we find that antiferromagnetism (single-magnon condensation) is suppressed by the AFM bipolaron condensate (SC state) because magnons do not condense individually, but as a component of a three-body bound state. This mechanism then illustrates the competition between antiferromagnetism and superconductivity: magnons can either condense individually to form an AFM state or become part of an AFM bipolaron that condenses into a SC state.

*Acknowledgments.* We thank Zhentao Wang, Sriram Shastri, and Andrey Chubukov for helpful discussions. C.D.B and S.-S.Z. are supported by funding from the Lincoln Chair of Excellence in Physics. W.Z. is supported by DOE NNSA through LANL LDRD program.

- 
- [1] P. W. Anderson, *Science* **235**, 1196 (1987).  
 [2] P. Anderson, *Mater. Res. Bull.* **8**, 153 (1973).  
 [3] L. Balents, *Nature (London)* **464**, 199 (2010).  
 [4] K. Takada, H. Sakurai, E. Takayama-Muromachi, F. Izumi, R. Dilanian, and T. Sasaki, *Nature (London)* **422**, 53 (2003).  
 [5] M. Ogata, *J. Phys. Soc. Jpn.* **72**, 1839 (2003).  
 [6] G. Baskaran, *Phys. Rev. Lett.* **91**, 097003 (2003).  
 [7] B. Kumar and B. S. Shastri, *Phys. Rev. B* **68**, 104508 (2003).  
 [8] H. Yokoyama, M. Ogata, and Y. Tanaka, *J. Phys. Soc. Jpn.* **75**, 114706 (2006).  
 [9] O. I. Motrunich and P. A. Lee, *Phys. Rev. B* **69**, 214516 (2004).  
 [10] Y. Nagaoka, *Phys. Rev.* **147**, 392 (1966).  
 [11] A. Mielke, *J. Phys. A: Math. Gen.* **24**, 3311 (1991).  
 [12] J. R. Schrieffer, X.-G. Wen, and S.-C. Zhang, *Phys. Rev. Lett.* **60**, 944 (1988).  
 [13] J. O. Haerter and B. S. Shastri, *Phys. Rev. Lett.* **95**, 087202 (2005).  
 [14] C. N. Sposetti, B. Bravo, A. E. Trumper, C. J. Gazza, and L. O. Manuel, *Phys. Rev. Lett.* **112**, 187204 (2014).  
 [15] F. T. Lisandrini, B. Bravo, A. E. Trumper, L. O. Manuel, and C. J. Gazza, *Phys. Rev. B* **95**, 195103 (2017).  
 [16] Note that the word “polaron” here is unrelated to lattice distortions, which are obviously absent in the purely electronic model that we are considering in this work.  
 [17] For  $t_1 > 0$ , the frustrated case corresponds to hole doping; for  $t_1 < 0$ , the frustrated case corresponds to electron doping.  
 [18] While a more realistic model should also include a second-nearest-neighbor hopping, the only purpose of including  $t_3$  is to vary the degree of kinetic energy frustration.  
 [19] See Supplemental Material at <http://link.aps.org/supplemental/10.1103/PhysRevB.97.140507> for technical details.  
 [20] For  $t_1 = 0$  and  $t_3 > 0$ , the triangular lattice is divided into four decoupled triangular sublattices with lattice constant  $2a$ . After rescaling the length scale by a factor  $1/\sqrt{3}$ , each sublattice

- becomes the same as the original triangular lattice with NN hopping. A small positive  $t_1$  term couples the two sublattices and yields a  $Q = 0$  bound state.
- [21] Here we are assuming that  $H$  and  $\mu$  take values such that the hole concentration equals twice the magnon concentration  $\rho_h = 2\rho_m$ .
- [22] V. L. Berezinskii, *Sov. Phys. JETP* **32**, 493 (1971).
- [23] V. L. Berezinskii, *Sov. J. Exp. Theor. Phys.* **34**, 610 (1972).
- [24] J. M. Kosterlitz and D. J. Thouless, *J. Phys. C* **6**, 1181 (1973).
- [25] Y. Yanase, M. Mochizuki, and M. Ogata, *J. Phys. Soc. Jpn.* **74**, 430 (2005).
- [26] Y. Nisikawa, H. Ikeda, and K. Yamada, *J. Phys. Soc. Jpn.* **73**, 1127 (2004).
- [27] W. A. Little, *Phys. Rev.* **134**, A1416 (1964).
- [28] V. L. Ginzburg, *Zh. Eksperim. i Teor. Fiz.* **47**, 2318 (1964).
- [29] W. Kohn and J. M. Luttinger, *Phys. Rev. Lett.* **15**, 524 (1965).
- [30] D. Fay and A. Layzer, *Phys. Rev. Lett.* **20**, 187 (1968).
- [31] V. L. Ginzburg, *Sov. Phys. Usp.* **19**, 174 (1976).
- [32] J. E. Hirsch and D. J. Scalapino, *Phys. Rev. B* **32**, 117 (1985).
- [33] R. Micnas, J. Ranninger, and S. Robaszkiewicz, *Rev. Mod. Phys.* **62**, 113 (1990).
- [34] A. V. Chubukov and J. P. Lu, *Phys. Rev. B* **46**, 11163 (1992).
- [35] A. V. Chubukov, *Phys. Rev. B* **48**, 1097 (1993).
- [36] M. E. Raikh, L. I. Glazman, and L. E. Zhukov, *Phys. Rev. Lett.* **77**, 1354 (1996).
- [37] R. Hlubina, *Phys. Rev. B* **59**, 9600 (1999).
- [38] J. Mráz and R. Hlubina, *Phys. Rev. B* **69**, 104501 (2004).
- [39] L. Isaev, G. Ortiz, and C. D. Batista, *Phys. Rev. Lett.* **105**, 187002 (2010).
- [40] S. Raghu, S. A. Kivelson, and D. J. Scalapino, *Phys. Rev. B* **81**, 224505 (2010).
- [41] A. S. Alexandrov and V. V. Kabanov, *Phys. Rev. Lett.* **106**, 136403 (2011).
- [42] S. Raghu and S. A. Kivelson, *Phys. Rev. B* **83**, 094518 (2011).
- [43] S. Raghu, E. Berg, A. V. Chubukov, and S. A. Kivelson, *Phys. Rev. B* **85**, 024516 (2012).
- [44] A. Hamo, A. Benyamini, I. Shapir, I. Khivrich, J. Waissman, K. Kaasbjerg, Y. Oreg, F. von Oppen, and S. Ilani, *Nature (London)* **535**, 395 (2016).
- [45] B. G. Levi, *Phys. Today* **56**, 15 (2003).
- [46] C. Becker, P. Soltan-Panahi, J. Kronjäger, S. Dörscher, K. Bongs, and K. Sengstock, *New J. Phys.* **12**, 065025 (2010).
- [47] J. Struck, C. Ölschläger, R. Le Targat, P. Soltan-Panahi, A. Eckardt, M. Lewenstein, P. Windpassinger, and K. Sengstock, *Science* **333**, 996 (2011).
- [48] J. Struck, M. Weinberg, C. Ölschläger, P. Windpassinger, J. Simonet, K. Sengstock, R. Höppner, P. Hauke, A. Eckardt, M. Lewenstein, and L. Mathey, *Nat. Phys.* **9**, 738 (2013).
- [49] I. Bloch, J. Dalibard, and W. Zwerger, *Rev. Mod. Phys.* **80**, 885 (2008).
- [50] D. Jaksch and P. Zoller, *Ann. Phys. (NY)* **315**, 52 (2005).